Desalination and Water Treatment
www.deswater.com

doi: 10.5004/dwt.2019.23332

138 (2019) 335–345
January

Preparation of textile sludge-derived activated carbons via KI and KOH activation for fast and efficient removal of methylene blue

Tang Shu Hui[a,b], Muhammad Abbas Ahmad Zaini[a,b,*]

[a]*Centre of Lipids Engineering and Applied Research (CLEAR), Ibnu-Sina Institute for Scientific and Industrial Research (ISI-SIR), Universiti Teknologi Malaysia, 81310 UTM Johor Bahru, Johor, Malaysia; emails: abbas@cheme.utm.my (M.A.A. Zaini); shtang1991@gmail.com (T.S. Hui)*
[b]*School of Chemical and Energy Engineering, Faculty of Engineering, Universiti Teknologi Malaysia, 81310 UTM Johor Bahru, Johor, Malaysia*

Received 13 June 2018; Accepted 22 October 2018

ABSTRACT

Textile sludge is a promising precursor of activated carbon. In this work, textile sludge-based activated carbons (TSACs) were prepared at different activation temperatures (400°C–800°C) and times (0.5, 1, and 2 h) using a mixture of potassium iodide (KI) and potassium hydroxide (KOH). The impregnation ratio of KI:KOH:textile sludge was fixed at 0.7:0.3:1. The effects of activation temperature and time on the methylene blue adsorption capacity were investigated, and response surface methodology was employed to optimize the process parameters. The TSACs were characterized for physicochemical properties. Results showed that the optimum activation conditions of 700°C for 1 h yield 17.9% of TSAC with an excellent maximum methylene blue adsorption capacity of 382 mg/g. The TSAC possessed high surface area, total pore volume, and microporosity of 1,180 m^2/g, 0.776 cm^3/g, and 56.5%, respectively. The isotherm study showed that the Langmuir model gave a good fit, indicating a monolayer adsorption. The adsorption kinetics was well described by the pseudo-second-order kinetics model, signifying that chemisorption may predominate, whereas the intraparticle diffusion model suggested that the pore diffusion is not the sole rate-limiting step. This study provides further understanding on the optimization of TSAC for dye wastewater treatment.

Keywords: Activated carbon; Activation; Methylene blue; Textile sludge

1. Introduction

With growing industrialization and population, preserving the quality of natural water bodies has become a worldwide challenging task. Each year, more than 7×10^5 tonnes of dyestuffs are produced with over 100,000 commercial dyes obtainable in the market [1]. Textile, paper, and leather manufacturing industries are the major source of dye wastewater pollution. The untreated effluents containing concentrated residual dye and other chemicals such as additives and surfactants are emitted directly into streams or water bodies. These pollutants can pose adverse effect to the environment and human health due to their toxicity, teratogenicity, carcinogenicity, and mutagenicity [2]. Methylene blue (MB) is a hazardous cationic dye that dissociates into a chloride anion and a cation in aqueous solution. The presence of dyes causes various health complications to human beings, microtoxicity in aquatic organisms, and impediment in the self-purification of water bodies [3]. Hence, it is pivotal to perform proper treatment on the industrial effluent prior to its discharge.

Adsorption using activated carbon is an effective and inexpensive technique owing to its simple design and operation, high efficiency and flexibility, insensitivity to toxic substances, and no sludge generation. Activated carbon is

* Corresponding author.

extensively used for eliminating pollutants in wastewater due to its good removal capacity, but the commercial activated carbons nowadays are costly and unsustainable. Hence, many efforts have been made to produce cost-effective activated carbon, particularly from agricultural and industrial wastes that are highly available like acorn shell [4], potato peels [5], oil palm ash [6], sisal fibre waste [7], sewage sludge [8] and textile sludge (TS) [9–11].

At present, the escalating sewage sludge generation from various industrial treatment plants is a critical encumbrance on the environmental sustainability and ecological health. Each year, approximately 3 million metric tonnes of sewage sludge is produced in Malaysia. Generally, the common sludge disposal methods include land-filling, land application, incineration, composting, and aerobic digestion [8]. However, these methods are only short-term solutions as they are expensive and induce secondary air and land pollution. Thus, converting industrial TS into activated carbon via chemical activation is an economical, effective, and environmentally friendly approach as this precursor is abundant and highly available, rich in volatile substances and has high carbon content.

In this study, textile sludge-based activated carbon (TSAC) was prepared via composite KI+KOH activation at optimum temperature and time. The novel composite activating agent has shown great potential in producing a negatively charged porous material [10]. Response surface methodology (RSM) was used to optimize the preparation conditions of TSAC on the MB adsorption capacity. The objectives of this work are (i) to study the effect of activation temperature and time on adsorption capacity of TSAC, (ii) to optimize the activation temperature and time on the adsorption capacity of TSAC using RSM, and (iii) to investigate the isotherm and kinetics of MB adsorption onto TSAC. This research would be a pivotal reference for industrial sludge resource utilization and contribute further understanding on dye wastewater treatment using TSAC.

2. Materials and methods

2.1. Materials

The raw material, industrial TS was supplied by American & Efird (Malaysia) in Johor state of Malaysia. Hydrochloric acid (30% HCl), potassium hydroxide (KOH) pellets, and MB (C0533-34048; M = 373.88 g/mol) were obtained from HmbG Chemicals, Germany. Potassium iodide (KI) was purchased from QREC (ASIA), Malaysia, while sodium hydroxide (96% NaOH) was obtained from Bendosen, Malaysia. All chemicals are of analytical reagent grade.

2.2. Preparation of activated carbon (TSAC)

TS was dried at 110°C for 48 h and was crushed to a particle size of 322 μm. A composite activating agent (KOH+KI) at fixed impregnation ratio of 0.7:0.3:1 (KI:KOH:TS) was used to prepare the TSACs. The mixture was stirred (120 rpm) and heated at 90°C for 1.5 h, and later was oven-dried at 110°C. The impregnated sample was activated at different temperatures, (T, 400°C–800°C) and times, (t, 0.5–2 h). The resultant products were soaked in HCl, and later were washed with distilled water until a constant solution pH was obtained. Then, the samples were oven-dried overnight and kept in a desiccator. The TSACs were labelled as TSAC-400-1 (T = 400°C, t = 1 h), etc. as summarized in Table 1.

Table 1
TSACs prepared at different activation temperatures and times

Sample	Activation temperature (°C)	Activation time (h)
TSAC-400-1	400	1
TSAC-500-1	500	1
TSAC-600-1	600	1
TSAC-700-1	700	1
TSAC-800-1	800	1
TSAC-700-0.5	700	0.5
TSAC-700-2	700	2

2.3. Characterization of activated carbon

The textural properties of activated carbons were determined by N_2 adsorption/desorption isotherms at 77 K with Brunauer–Emmett–Teller (BET) technique using a NOVA 2200e (Quantachrome Instruments, USA). The images of microstructure and intrastructures of activated carbons were analyzed using SEM-50 (Philips, Holland). The surface functional groups were detected by a spectrum GX FT-IR (PerkinElmer, USA).

2.3.1. Bulk density

A measuring cylinder was first weighed. The TSAC was placed into this cylinder and was reweighed. The bulk density was calculated using the following expression:

$$\text{Bulk density } (\text{g/L}) = \frac{W_2 - W_1}{V} \quad (1)$$

where W_1 = weight of measuring cylinder (g), W_2 = weight of measuring cylinder + its contents (g), and V = volume of the content in measuring cylinder (L).

2.3.2. Ash content

A fixed amount of TSAC was dried at 110°C overnight and was later carbonized at 900°C for 2 h. The sample was left to cool in a desiccator, and the final weight was recorded. The ash content (dry basis) was calculated as follows:

$$\text{Ash content } (\%) = \frac{W_f}{W_i} \times 100 \quad (2)$$

where W_i is the initial weight of dry sample and W_f is the final weight of sample after carbonization.

2.3.3. Moisture content

A fixed amount of TSAC was left outside for a day. It was later dried in oven at 110°C for 24 h and left to cool inside a

desiccator. The final weight was recorded. The equation of moisture content is shown as follows:

$$\text{Moisture content}\ (\%) = \frac{W_i - W_f}{W_i} \times 100 \tag{3}$$

where W_i is the initial weight of sample (wet) and W_f is the final weight of dry sample.

2.4. Adsorption experiments

Stock solution of 1,000 mg/L was prepared, and subsequent dilution was performed to get dye solution of desired concentrations. Batch adsorption was carried out in 150 mL conical flasks containing 0.05 g of TSAC and 50 mL of MB solution of known initial concentrations (5–600 mg/L) at 25°C. The pH of the solutions was left unchanged. The solid-solution mixture was agitated at 120 rpm and maintained at room temperature for 72 h. The equilibrium concentration of MB in the solution was measured using a Halo VIS-10 visible spectrophotometer (Dynamica, Australia) at λ = 603 nm. Dilutions of dye solution were carried out whenever necessary. The adsorption capacity of TSACs at equilibrium was calculated according to the equation as follows:

$$q_e = \frac{C_o - C_e}{m} \times V \tag{4}$$

where q_e (mg/g) is the amount of dye adsorbed at equilibrium, C_o and C_e (mg/L) are the initial concentration and equilibrium concentration of dye solution, respectively, V (L) is the volume of dye solution, and m (g) is the mass of dry adsorbent [10].

The equilibrium data were fitted to Langmuir, Freundlich, Temkin, and Dubinin–Radushkevich (D–R) isotherm models as follows:

$$q_e = \frac{q_m b C_e}{(1 + bC_e)} \tag{5}$$

where b (L/mg) is the Langmuir isotherm constant and q_m (mg/g) is the maximum monolayer capacity.

$$q_e = k_F (C_e)^{\frac{1}{n}} \tag{6}$$

where k_F ((mg/g) (L/mg)$^{1/n}$) is the Freundlich isotherm constant related to adsorption capacity and 1/n reflects the adsorption intensity.

$$q_e = \frac{RT}{b_T} \ln A_T C_e \tag{7}$$

$$B = \frac{RT}{b_T} \tag{8}$$

where R is the gas constant (8.314 J/mol·K), T (K) is the absolute temperature, b_T is the variation of adsorption energy, B (J/mol) is the Temkin constant corresponding to the heat of sorption, and A_T (L/mg) is the equilibrium binding constant related to the maximum binding energy [2,21].

$$q_e = Q_s \exp(-K_{\text{ad}} \varepsilon^2) \tag{9}$$

$$\varepsilon = RT \ln\left(1 + \frac{1}{C_e}\right) \tag{10}$$

$$E_a = \frac{1}{\sqrt{2K_{\text{ad}}}} \tag{11}$$

where Q_s (mg/g) is the theoretical isotherm saturation capacity, K_{ad} (mol^2/kJ^2) is the D–R isotherm constant, E_a (kJ/mol) is the free energy per molecule of adsorbate, and ε (kJ/mol) is the D–R isotherm constant [8].

The adsorption kinetics was performed at concentrations of 100 and 450 mg/L. A total of 0.05 g of activated carbon was added into 50 mL of MB solution of known concentrations. The mixture was agitated in a shaker at room temperature and 120 rpm for 72 h. The concentration was measured at different time intervals. The kinetics models, namely the pseudo-first-order (Eq. (12)), pseudo-second-order (Eq. (13)), and intraparticle diffusion (Eq. (14)) models were used to evaluate the rate of adsorption.

$$q_t = q_e \left(1 - e^{-k_1 t}\right) \tag{12}$$

$$q_t = \frac{k_2 q_e^2 t}{1 + q_e k_2 t} \tag{13}$$

$$q_t = k_{\text{diff}} t^{0.5} + C \tag{14}$$

where q_t (mg/g) is the amount of dye adsorbed at time t, t (h) is the period of adsorption, k_1 (h^{-1}) is the rate constant for pseudo-first-order sorption, k_2 (g/mg h) is the rate constant for pseudo-second-order sorption, k_{diff} (mg/g h$^{0.5}$) is the diffusion coefficient for intraparticle sorption, and C (mg/g) is the intraparticle diffusion constant.

2.5. Experimental design and optimization

RSM is a group of mathematical and statistical approaches, which is extensively applied in the industrial field to design, formulate, develop, improve, and optimize new scientific processes [12]. RSM is crucial in the analysis and modelling of problems involving an output response affected by some independent variables. Design-Expert 7.0 software was used to perform the experimental design, mathematical modelling, and optimization. In this study, the RSM historical data design was chosen in order to generate a custom design and import the existing data. Activation time and temperature are independent variables, while the adsorption

capacity (high priority) is the output responses. The coefficient was obtained via multiple regression analysis, and the response was predicted using the model equation.

3. Results and discussion

Industrial TS is a waste product of biological wastewater treatment process and scheduled for solid disposal. It can be recycled as a precursor of activated carbon. TS is made up of 42.3% carbon, 5.5% hydrogen, 45.7% oxygen, and 16% inorganic materials [10].

KOH is a popular activating agent, which is widely used to produce microporous materials. Yet, it has certain drawbacks including lower product yield and toxicity of KOH [13]. Besides, KOH may not be effective in activating precursor with high ash content (e.g., sewage sludge) due to the possible clogging of pores by inorganic materials. Moreover, TS activation using $ZnCl_2$, H_2SO_4, and KCl had shown low surface area (~222 m^2/g) and poor MB adsorption performance (~13 mg/g) [11]. With the novel composite activating agent KI+KOH, the surface area and mesoporosity of the TSAC can be further enhanced as a result of pore drilling and widening of micropores. The potential of KI+KOH is evident, as reported by Tang and Zaini [10]. The surface area, yield, and adsorption capacity of the KI+KOH-activated TSACs are superior compared with that of KOH- and KI-activated TSACs. TSAC was prepared via KI+KOH chemical activation at fixed impregnation ratio of 0.7:0.3:1 (KI:KOH:TS) as it was found to be the best mass ratio from a previous study [10].

3.1. Characteristics of TSAC

The pH of solution affects the adsorption process as it influences the degree of ionization of adsorbents and functional groups. MB has a pKa of 3.14, therefore it exists in its cation form and participates in the electrostatic interaction with TSAC. In this work, the pH of dye solution was found to vary between 4.34 and 5.55, whereas the pH values of TSACs are in the range of 3.90 and 4.25. It was reported that the pH_{pzc} of TSACs are lesser than the pH of TSACs [10], indicating the negatively charged surface of TSAC in aqueous solution owing to the presence acidic functional groups. The pH of dye solution is higher than the pH_{pzc} of TSAC and pKa of MB, resulting in a negative net surface charge of TSAC, which in turn creates the electrostatic attraction between the positively charged MB (solution pH > pKa, MB) and the negatively charged surface of TSAC (solution pH > pH_{pzc}). In other words, the adsorption of MB onto TSAC is a favourable process with good affinity.

Table 2 summarizes the pH, bulk density, ash content, and moisture content of TSACs. The ash content and moisture content of TSAC are ranging from 13.4% to 57.1% and 14.6% to 27.6%, respectively. The moisture content generally increases with surface area, but TSAC-700-2 has the highest moisture content mostly due to its lower microporosity (22%) which allows it to be more prone to moisture exposure. It was found that TSAC-800-1 has the highest ash content of 57% because high activation temperature promotes gasification of carbon into CO and CO_2 which results in decreasing amount of organic compound (in TSAC) while the content of inorganic compound remains relatively fixed. Besides that, the TSACs also have low bulk density, which is in between 0.237 and 0.324 g/L, owing to the presence of micropores and mesopores. The pH of the TSACs was found to decrease with increasing activation temperature and time, owing to the destruction of acidic functional groups and volatilization during carbonization.

Fig. 1 shows the surface morphology of TSAC-700-1. The SEM images exhibit the extremely porous surface with the formation of both micropores and mesopores, indicating

Table 2
pH, bulk density, ash content, and moisture content of TSACs

Sample	pH	Ash content (%)	Moisture content (%)	Bulk density (g/L)
TSAC-600-1	3.96	27.0	14.6	0.276
TSAC-700-1	4.05	13.4	19.6	0.300
TSAC-800-1	4.25	57.1	18.9	0.267
TSAC-700-0.5	3.90	39.7	16.7	0.324
TSAC-700-2	4.19	17.6	27.6	0.237

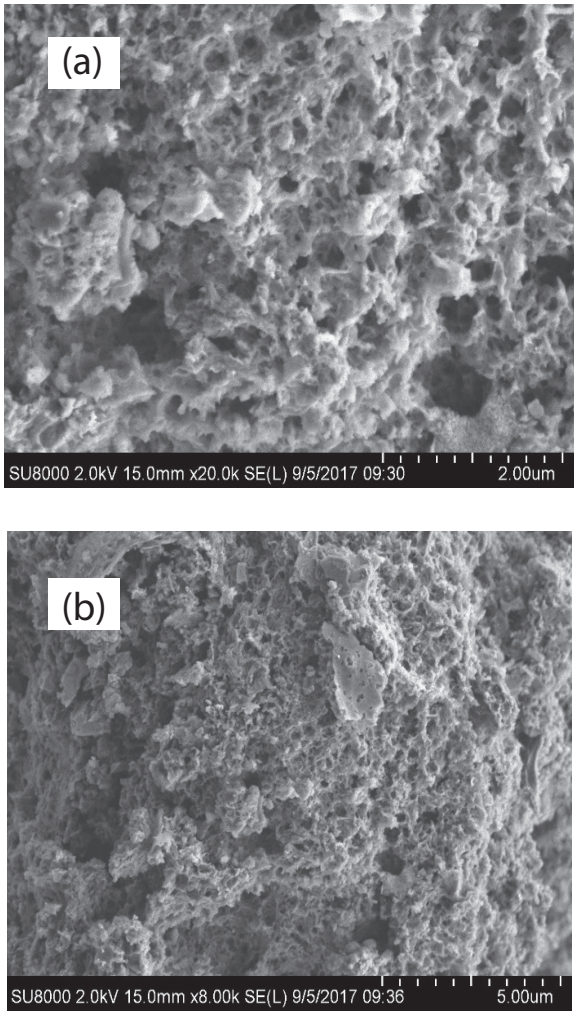

Fig. 1. SEM images of TSAC-700-1 at different magnifications (a) 20,000 and (b) 8,000.

that KI+KOH activation had effectively taken place. During pyrolysis, the gasification, pore drilling, and pore widening process give rise to the development of irregular-shaped pores with various pore sizes of wide distribution. The presence of micropores and mesopores assists greatly in the removal of larger dye molecules. The highly porous surface of TSAC-700-1 is in accordance with its high surface area and adsorption capacity of 1,180 m^2/g and 382 mg/g, respectively.

Fig. 2 shows the Fourier-transform infrared (FTIR) spectra of TS and TSAC. Multiple peaks in the spectrum of TS denote the presence of volatile matters. The broadband at 3,292 cm^{-1} is attributed to the stretching of hydroxyl (O–H) groups due to hydroxyl-containing structures (alcohol, phenol, and carboxylic acid) and moisture in the raw material [4]. The small peak located at 2,922 cm^{-1}corresponds to the stretching of C–H in aliphatic chains [3], while two narrow peaks at 1,717 and 1,638 cm^{-1} are ascribed to the stretching vibration of carbonyl (–C=O) group. Peaks at 1,524, 1,408, 1,263, and 731 cm^{-1} represent the N–H bonds in primary and secondary amines, phenolic –OH, C–O, and C–X (X = F, Cl, Br, and I) bonds, respectively [10]. Two peaks at 1,097and 1,030 cm^{-1} are related to C–N stretching vibrations. Upon KI and KOH activation, only five prominent peaks were observed on TSAC, signifying the liberation volatiles during carbonization. The peaks at 3,357, 2,105, 1,587, and 1,037 cm^{-1} can be assigned to O-H, C–O, C=O, and C–N stretching [8], while the tiny peak at 2,388 cm^{-1} corresponds to the physisorbed CO_2.

Table 3 shows that the increase in activation temperature generally results in the increment of surface area, average pore diameter, and pore volume but causes a drop in microporosity. A higher temperature (i) promotes reaction of C–KOH and C–KI and (ii) intensifies the volatilization and gasification of TS. The rudimentary pore network structure is initially formed in the char after volatilization, while the reaction of C–KOH and C–KI further develops new micropores and mesopores. Metallic K from KI and KOH intercalates into carbon lattices, causing the lattice to expand and enlarge. The intercalated K and other compounds were then removed by washing with HCl and distilled water, therefore leaving behind the expanded porous carbon network. Nevertheless, the decrease in microporosity is most likely attributed to the pore widening and opening of existing micropores, which increases the pore diameter and pore volume. These reactions occur concurrently and greatly affect the textural properties of TSAC. Above optimum activation condition, the surface area and microporosity of TSAC decreased because the existing micropores and mesopores collapse and merge to form more mesopores and macropores due to flimsy pore walls. As a result, the mesopore volume and average pore diameter of TSAC increased.

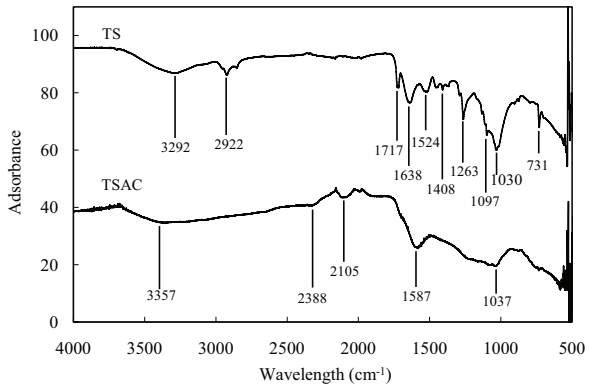

Fig. 2. FTIR spectrum of textile sludge (TS) and TSAC.

3.2. Effects of activation temperature and time on TSAC yield and MB adsorption

Activation temperature and time influence the yield, physical properties, and adsorption capacity of adsorbents. Fig. 3(a) shows that the yield decreased from 29.6% to 5.4% with increasing activation temperature from 400°C to 800°C. This is due to the intensive volatilization, excess carbon burn-off, and decomposition of molecular organic compound, which occurred at higher temperature.

From Fig. 3(a), it can also be seen that the maximum adsorption capacity (q_m) increased from 25 to 382 mg/g with increasing activation temperature until 700°C, but decreased slightly beyond this temperature. The good adsorption capacity is closely attributed to the enhanced surface area and micropore volume as shown in Table 3. However, the decline in q_m at activation temperature of 800°C could be caused by the diminished adsorption sites as the surface area of TSAC decreased from 1,180 to 1,103 m^2/g. Besides, the destruction of surface functional groups beyond 700°C may also contribute to the lower q_m. Thus, it was discovered that 700°C is the best activation temperature, which yielded the highest q_m and surface area.

In general, the activation time is inversely proportional to the yield of activated carbon. The yield decreased from 17.9% to 2.2% as the activation increased from 0.5 to 2 h at

Table 3
Textural properties and pH of TSACs

Sample	S_{BET} (m^2/g)	V_T (cm^3/g)	V_{Mi} (cm^3/g)	V_{Me} (cm^3/g)	R_{Mi} (%)	D_p (nm)
TSAC-600-1	834	0.507	0.301	0.206	59.3	2.61
TSAC-700-1	1,180	0.776	0.438	0.338	56.5	2.79
TSAC-800-1	1,103	0.815	0.395	0.42	48.5	3.11
TSAC-700-0.5	862	0.581	0.327	0.254	56.4	2.86
TSAC-700-2	175	0.253	0.056	0.197	22.0	5.90

S_{BET}, BET specific surface area; V_T, total pore volume; V_{Mi}, micropore volume; V_{Me}, mesopore volume; R_{Mi}, microporosity; D_p, average pore diameter.

a fixed activation temperature of 700°C. This is associated to the presence of activating agent, which was incorporated into carbon framework burning out obstructions within the TS while developing the pore network due to the longer pyrolysis time.

The relationship between activation time and q_m at activation temperature of 700°C was shown in Fig. 3(b). It can be seen that the q_m increased from 250 to 382 mg/g as the activation time increased from 0.5 to 1 h. This is because the activation time of 1 h is sufficient to allow the maximum development of pores and consequently increases the surface area of TSAC from 862 to 1,180 m^2/g (Table 3), thus enhancing the q_m. Even so, the q_m plunged from 382 to 40 mg/g when the activation time increased from 1 to 2 h, owing to the significant drop in surface area from 1,180 to 175 m^2/g (Table 3) which may be caused by the destruction and clogging of existing pores. The effect of activation time on other textural properties such as pore diameter, pore volume, and microporosity is less prominent and generally has almost the same trend as that shown in Fig. 3(b). Therefore, based on the experimental data, it was found that the TSAC prepared at 700°C and 1 h (TSAC-700-1) possesses the highest surface area and q_m of 1,180 m^2/g and 382 mg/g, respectively. The optimum activation conditions of 700°C and 1 h were further validated via RSM optimization.

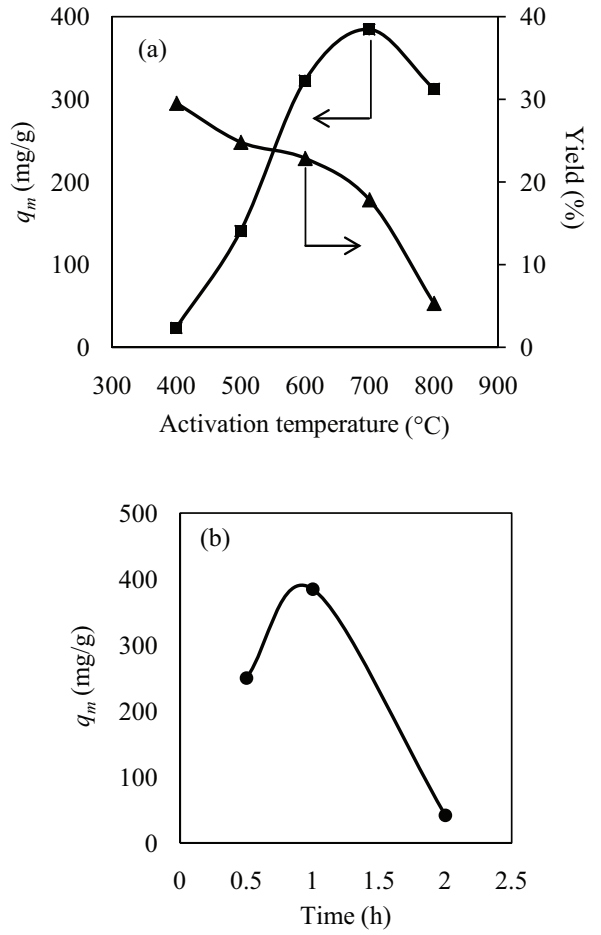

Fig. 3. (a) Effect of activation temperature on yield and q_m and (b) effect of activation time of TSAC-700 on q_m.

3.3. RSM for process optimization

Design-Expert 6.0.4 was used to carry out the response surface analysis. The regression model was applied to fit the two factors (A = activation temperature and B = activation time) with MB removal capacity (Y) as the response output. The regression model test analysis of variance with 95% confidence level (α = 0.05) was employed. The quadratic regression equation below shows an empirical relationship between the activation temperature (A), activation time (B), and MB removal capacity (Y):

$$Y = 353.33 + 103.31A + 2.92B - 196.92A^2 - 135.88B^2 - 163.34AB \quad (15)$$

The model F-value of 4.51 implies that the model is significant. There is only a 4.72% chance that a 'Model F-Value' this large could occur due to noise. The correlation coefficient of R^2 = 0.7897 signifies a suitable fit of the model, and good correlation between the two variables and the response output. From Eq. (15), there is interaction between A and B which results in various interaction terms including AB and also single-factor terms A^2 and B^2. From Table 4, the primary parameter A for the model is significant (with P value of 0.03), and it indicates that the activation temperature plays an important role in the MB adsorption capacity of TSAC. The statistical interactions and curvilinear relationship between the variables are presented in Fig. 4(a).

Table 4 exhibits the significance of the data elicited by regression model analysis. The model is significant when

Table 4
ANOVA results of the quadratic regression model for methylene blue removal

Source	Sum of square	Degrees of freedom	Mean square	F value	P value
Model	1.578×10^5	5	31,560	4.51	0.0472
A	54,390	1	54,390	7.77	0.0317
B	36.53	1	36.53	0.005	0.9448
A^2	1.157×10^5	1	1.157×10^5	16.52	0.0066
B^2	28,250	1	28,250	4.03	0.0913
AB	34,640	1	34,640	4.95	0.0678
Residual	42,010	6	7,002	–	–
Total	1.998×10^5	11	–	–	–

$0.01 < P < 0.05$, or else the model is insignificant when $P > 0.05$. The P value of the equation is 0.0472 as shown in Table 4, and this suggests that the model or coefficient is significant. Besides, the significance for the regression model can also be seen through the low probability value in the F-test. Moreover, the normal plot of residuals (Fig. 4(b)) shows that the residual error is low, and the experimental data and the predicted values are close. Thus, the model can be applied for the optimization of the preparation conditions of TSAC. The optimization was performed using Design-Expert by setting the activation temperature and time to be 'in range', and the maximum adsorption capacity was set to be maximum with highest priority. It was found that the optimal conditions for the highest maximum adsorption capacity of 370.8 mg/g are 668.6°C and 1.1 h with desirability of 0.962. These values are close to the experimental ones (700°C, 1 h) with minimal relative errors of 4.5% (activation temperature) and 10% (activation time), respectively. In other words, the preparation conditions of 700°C and 1 h are practical and reliable.

3.4. Equilibrium adsorption

Adsorption isotherm is crucial in describing the distribution of adsorbed molecules between the solid phase and the bulk liquid phase at equilibrium [14]. Single-component isotherm models such as Langmuir and Freundlich are widely used in various studies involving contaminant adsorption from liquid solution. The Langmuir isotherm assumes monolayer adsorption at specific homogeneous sites within the adsorbent, constant adsorptional energy, identical and energetically equivalent sites, and the absence of interaction between molecules adsorbed on neighbouring sites [15]. On the other hand, the Freundlich isotherm is based on non-ideal and reversible multilayer adsorption with varied distribution of adsorption heat and affinities over the heterogeneous surface [16].

Fig. 5 shows the equilibrium adsorption of MB onto TSAC-700-1. Generally, the adsorption at equilibrium (q_e) initially surges with increasing equilibrium concentration (C_e), but slowly becomes a horizontal plane at higher C_e, indicating that the saturation point is attained. At lower C_e, the number of MB dye molecules is the limiting factor, while at higher C_e, the number of accessible adsorption sites becomes the restricting factor. The models parameters are presented in Table 5. The Langmuir model gave the best fit with high correlation coefficient (R^2) and low root-mean-square error (RMSE) for all the prepared samples, signifying the monolayer adsorption of MB onto TSAC. Besides, the values of $1/n$ of Freundlich model are all less than 1, denoting an ideal Langmuir isotherm [17], thus confirming the good applicability of Langmuir model to describe the equilibrium data. From Table 5, TSAC-700-1 possesses the highest Langmuir maximum adsorption capacity (382 mg/g), followed by TSAC-600-1 (321 mg/g) and TSAC-800-1 (315 mg/g). In addition, the high values of b indicate a good affinity of TSAC towards MB dye molecules.

The adsorption equilibrium data were also fitted to Temkin and D–R isotherm models. Temkin isotherm reports the chemisorption process as electrostatic interaction and assumes that the indirect adsorbate–adsorbate interactions cause the adsorption energy to decrease linearly with the surface coverage [8,10]. From Table 6, the satisfactory R^2 and generally high B values (>20 J/mol) of Temkin model indicate a possible electrostatic interaction between MB and TSAC to a certain extent. The D–R isotherm is mainly used to describe the mechanism of adsorption by the Gaussian energy distribution onto a heterogeneous surface [18]. The D–R isotherm

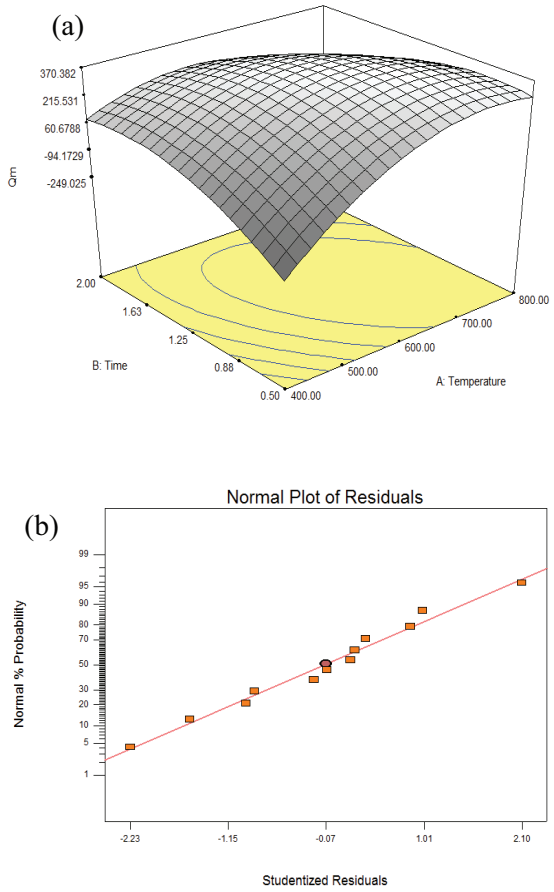

Fig. 4. (a) Response surface curve of MB removal and (b) normal probability and internally studentized residuals for methylene blue removal.

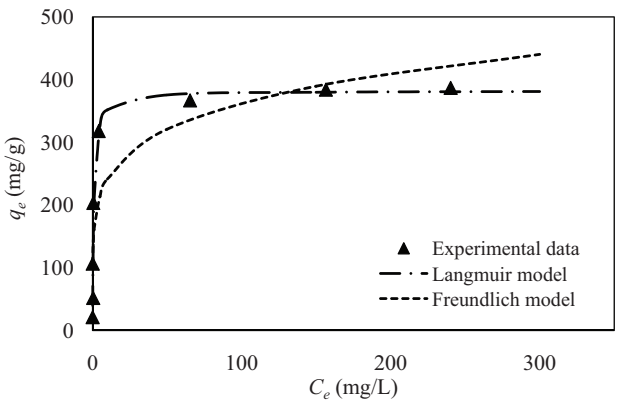

Fig. 5. Adsorption isotherm of MB onto TSAC-700-1 (experimental conditions: C_o = 20–600 mg/L, contact time = 72 h, T = 25°C, and agitation speed = 120 rpm).

Table 5
Langmuir and Freundlich constants

Sample	Langmuir model				Freundlich model			
	q_m (mg/g)	b (L/mg)	R^2	RMSE	n	k_F ((mg/g)(L/mg)$^{1/n}$)	R^2	RMSE
TSAC-400-1	25.1	0.82	0.947	2.29	5.11	11.1	0.725	4.91
TSAC-500-1	118	0.97	0.517	33.8	5.89	52.7	0.584	31.2
TSAC-600-1	321	1.23	0.931	34.4	5.76	132.9	0.838	53.0
TSAC-700-1	382	1.16	0.917	44.4	5.66	160.9	0.798	69.8
TSAC-800-1	315	1.10	0.911	37.1	4.97	130.6	0.776	59.3
TSAC-700-0.5	250	0.60	0.947	22.9	5.51	95.5	0.843	4.58
TSAC-700-2	40	3.06	0.813	3.67	12.42	26.5	0.711	40

Table 6
Temkin and Dubinin–Radushkevich (D–R) constants

Sample	Temkin model					D–R model				
	b_T	B (J/mol)	A_T (L/mg)	R^2	RMSE	K_{ad} (mol^2/kJ^2)	Q_s (mg/g)	E_a (kJ/mol)	R^2	RMSE
TSAC-400-1	691	3.64	17.9	0.818	3.97	2×10^{-7}	22.9	1.58	0.991	1.09
TSAC-500-1	174	14.5	34.0	0.582	31.3	2×10^{-7}	110	1.58	0.565	32.3
TSAC-600-1	60.3	36.6	46.8	0.898	35.8	5×10^{-8}	242	3.16	0.815	72.3
TSAC-700-1	55.8	45.2	43.1	0.867	56.2	7×10^{-8}	311	2.67	0.845	68.4
TSAC-800-1	61.2	41.2	31.2	0.848	48.5	4×10^{-8}	184	3.54	0.710	89.7
TSAC-700-0.5	80.3	31.4	17.1	0.917	28.8	1×10^{-7}	218	2.24	0.876	42.9
TSAC-700-2	887	2.84	8846	0.758	4.18	6×10^{-8}	39.5	2.89	0.801	3.83

also exhibits satisfactory R^2 and the E_a values in the range of 1–8 kJ/mol, suggesting a physical adsorption [8]. Therefore, it can be said that the adsorption of MB onto TSAC is a combination of chemisorption and physisorption, whereby physisorption can occur on the layer on which chemisorption had taken place.

3.5. Adsorption kinetics

The effect of contact time on the adsorption of MB was studied at concentrations of 100 and 450 mg/L, as shown in Fig. 6. Overall, the kinetics behaviour consists of three phases – a rapid initial adsorption, followed by a significantly slower adsorption and finally a gradual equilibrium adsorption is achieved. In the first phase, the very steep line observed in Fig. 6 is associated with fast adsorption rate due to large numbers of available active sites. After some time, the adsorption capacity started to decline as the active sites are slowly saturated, and repulsion (desorption) may occur between the adsorbed dye molecules on TSAC and the free-moving dyes in the bulk solution. Eventually, the adsorption reached an equilibrium state, at which the rate of adsorption is equal to the rate of desorption. The superior affinity of TSAC-700-1 towards MB dye molecules was also noticed through rapid adsorption rates during kinetics study. Fig. 6(b) shows that TSAC-700-1 took only 5 min to achieve adsorption equilibrium at C_o = 100 mg/L, while it removed 170 mg/g within 5 min at C_o = 450 mg/L. This finding further affirms the high values of Langmuir constant b (Table 5) which is closely related to the affinity of adsorbent to adsorbate.

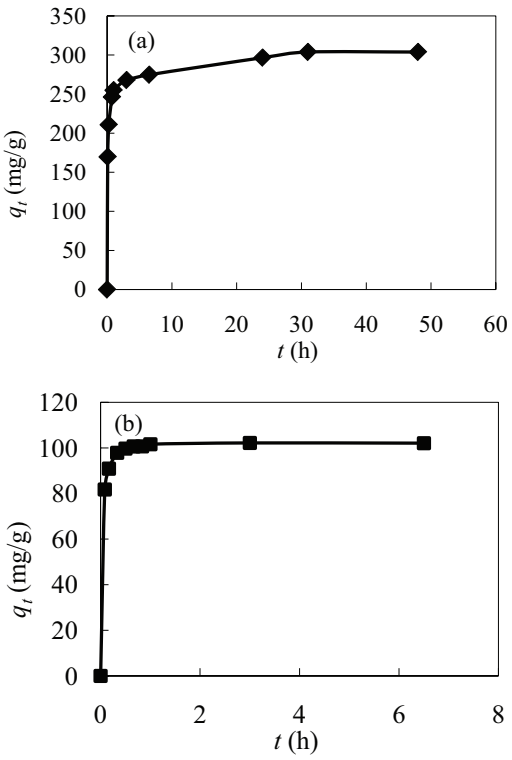

Fig. 6. Effect of contact time on methylene blue removal by TSAC-700-1 at (a) C_o = 450 mg/L and (b) C_o = 100 mg/L (experimental conditions: T = 25°C and agitation speed = 120 rpm).

The pseudo-first-order and pseudo-second-order kinetics models were used to evaluate the rate of adsorption. The pseudo-first-order model assumes that the adsorption rate is proportional to the amount of solute adsorbed from the bulk solution and physical adsorption is involved, whereas the pseudo-second-order is based on chemisorption through ion exchange or electron sharing between the adsorbent and adsorbate via valency forces [5]. It can be seen from Table 7 that the kinetics data are well fitted to pseudo-second order, suggesting that chemisorption may prevail over physisorption and the model can be used to predict the adsorption of MB onto TSAC. Table 7 also shows that the pseudo-second-order rate constant k_2 is greater at MB concentration of 100 mg/L compared with 450 mg/L. This is because of the rapid adsorption rate, high number of accessible adsorption sites, and less restriction among MB molecules in bulk solution at lower concentration.

The adsorption mechanism often occurs in three steps – adsorption of adsorbate onto adsorbent surface, film diffusion via the boundary layer, and intraparticle diffusion. The slowest step is considered the rate-limiting step for batch adsorption system. For further understanding of the effect of diffusion on adsorption mechanism, the intraparticle diffusion model was employed to fit the kinetics data. It is based on the assumptions that (i) the sole rate-limiting step is intraparticle diffusion, (ii) the boundary layer diffusion or film diffusion is insignificant [19], (iii) the pattern of diffusion is radial, and (iv) constant pore diffusivity [20]. A straight line elicited from the plot of q_t against $t^{0.5}$ that passes through the origin implies the pore diffusion or intraparticle diffusion is the sole rate-limiting step.

Table 7
Parameters of the kinetics models of TSAC-700-1

Models	Parameter	Concentration	
		100 mg/L	450 mg/L
	Exp. q_e (mg/g)	102	304
Pseudo-first order	Cal. q_e (mg/g)	100	276
	k_1 (h^{-1})	19	8.97
	R^2	0.909	0.877
	RMSE	2.38	25.6
Pseudo-second order	Cal. q_e (mg/g)	103	286
	k_2 (g/mg h)	0.44	0.05
	R^2	0.998	0.983
	RMSE	0.613	14.8
Intraparticle diffusion	k_{diff} (mg/g $h^{0.5}$)	5.84	15.2
	C (mg/g)	91.7	218
	R^2	0.886	0.78
	RMSE	5.43	24.9

Fig. 7 shows multilinear plots with three and two linear segments. These plots did not pass through the origin and had different intercepts. Thus, the pore diffusion is not the only rate-controlling step at the initial stage of batch adsorption. At the initial steep phase, the film diffusion may have taken control from 0 to 1 h for 450 mg/L, and from 0 to 0.6 h for 100 mg/L, indicating the external mass transfer effects. The second gradual phase attributed the intraparticle diffusion, while the third phase (exist in higher concentrations) represents adsorption equilibrium. Although there were two or three processes governing the MB sorption rate, only one predominates at specific time. Similar trend of the intraparticle diffusion plot was also reported by Hameed and El- Khaiary [20]. Furthermore, the positive value of C listed in Table 7 suggests the extent of film-diffusion controlling and rapid adsorption, while negative value of C indicates that the intraparticle diffusion is obstructed by the thick boundary layer [10].

3.6. Comparison of MB removal with other adsorbents

The adsorption capacity and surface area of TSAC developed in this work were compared with various MB adsorbents. Table 8 summarizes the adsorption performance of various adsorbents in the removal of MB. The TSAC prepared via KI+KOH activation (700°C, 1 h) exhibits a superior surface area of 1,180 m^2/g and MB

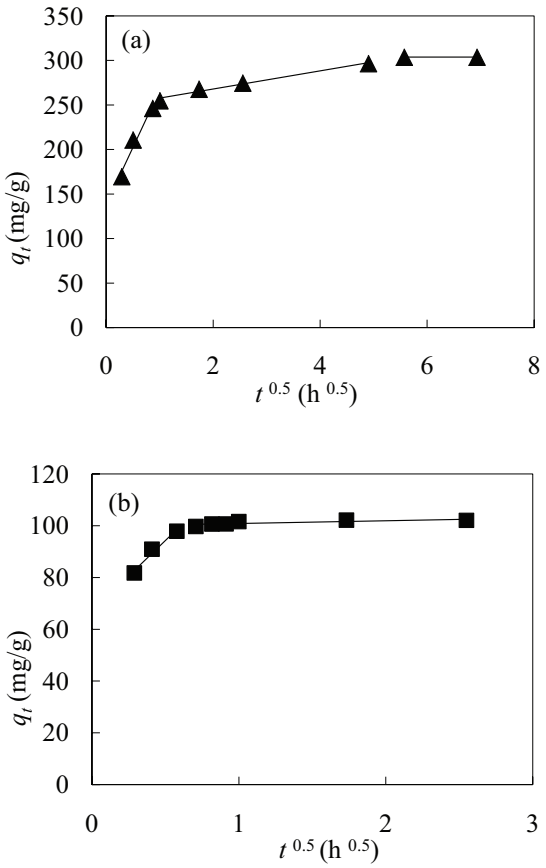

Fig. 7. Intraparticle diffusion plots for methylene blue adsorption at concentrations of (a) 450 mg/L and (b) 100 mg/L.

Table 8
Comparison of MB adsorption by various adsorbents

Adsorbent	Activating agent	Surface area (m^2/g)	Adsorption capacity (mg/g)	Reference
Textile sludge-activated carbon	KI+KOH	1,180	382	This study
Textile sludge-activated carbon	H_2SO_4	222	13.3	[11]
Activated carbon-alginate beads	$ZnCl_2$	890	287	[21]
Sewage sludge-derived biochar	–	25	24.1	[8]
Magnetic acorn shell-activated carbon	$ZnCl_2$	940	357	[4]
Acorn shell-activated carbon	$ZnCl_2$	870	330	
Zeolite–activated carbon composite	NaOH	615	143	[6]
Maize silk powder	–	0.00207	234	[3]
Chitosan-activated carbon	NaOH	318	122	[22]
Sawdust char	–	–	31.2	[2]
Sawdust-activated carbon	H_3PO_4	–	21.9	
Sawdust-activated carbon	$ZnCl_2$	–	37.0	
Textile sludge-activated carbon	KI	191	90.9	[9]

adsorption capacity of 382 mg/g as compared with other recently reported adsorbents in literature. It shows that the KI and KOH composite is a promising activating agent for precursor with high ash content, and the resultant TSAC is an effective adsorbent for the removal of MB.

4. Conclusion

The preparation conditions of TSAC were optimized using RSM. The experimental data fitted to the quadratic regression model with correlation coefficient (R^2) of 0.8001 and P value of 0.0411. This shows that the model is significant and the preparation conditions of TSAC had been optimized. The experimental and optimized data display small relative error indicating that the preparation conditions of 700°C and 1 h are practical and reliable. This finding is further validated by the high surface area (1,180 m^2/g) and superior maximum adsorption capacity (382 mg/g) of TSAC-700-1. Besides, the Langmuir isotherm and pseudo-second-order kinetics models are good fits to the equilibrium and kinetics data, respectively, signifying the monolayer chemisorption of MB onto TSAC may predominate. It was also found that the pore diffusion is not the sole rate-limiting step. In short, this research would be a pivotal reference for industrial sludge resource utilization and contribute further understanding on dye wastewater treatment using TSAC.

Acknowledgment

The authors would like to express appreciation for the support of UTM-Flagship Grant #03G70.

References

[1] R. Kant, Textile dyeing industry an environmental hazard, Nat. Sci., 4 (2012) 22–26.
[2] S. Agarwal, I. Tyagi, V.K. Gupta, N. Ghasemi, M. Shahivand, M. Ghasemi, Kinetics, equilibrium studies and thermodynamics of methylene blue adsorption on *Ephedra strobilacea* saw dust and modified using phosphoric acid and zinc chloride, J. Mol. Liq., 218 (2016) 208–218.
[3] S.M. Miraboutalebi, S.K. Nikouzad, M. Peydayesh, N. Allahgholi, L. Vafajoo, G. McKay, Methylene blue adsorption via maize silk powder: kinetic, equilibrium, thermodynamic studies and residual error analysis, Process Saf. Environ., 106 (2017) 191–202.
[4] E. Altıntıg, H. Altundag, M. Tuzen, A. Sarı, Effective removal of methylene blue from aqueous solutions using magnetic loaded activated carbon as novel adsorbent, Chem. Eng. Res. Des., 122 (2017) 151–163.
[5] G.Z. Kyzas, E.A. Deliyanni, Modified activated carbons from potato peels as green environmental-friendly adsorbents for the treatment of pharmaceutical effluents, Chem. Eng. Res. Des., 97 (2015) 135–144.
[6] W.A. Khanday, F. Marrakchi, M. Asif, B.H. Hameed, Mesoporous zeolite–activated carbon composite from oil palm ash as an effective adsorbent for methylene blue, J. Taiwan Inst. Chem. Eng., 70 (2017) 32–41.
[7] M. Dizbay-Onat, U.K. Vaidya, C.T. Lungu, Preparation of industrial sisal fiber waste derived activated carbon by chemical activation and effects of carbonization parameters on surface characteristics, Ind. Crops Prod., 95 (2017) 583–590.
[8] S. Fan, Y. Wang, Z. Wang, J. Tang, J. Tang, X. Li, Removal of methylene blue from aqueous solution by sewage sludge-derived biochar: adsorption kinetics, equilibrium, thermodynamics and mechanism, J. Environ. Chem. Eng., 5 (2017) 601–611.
[9] S.H. Tang, M.A.A. Zaini, Isotherm studies of methylene blue adsorption onto potassium salts-modified textile sludge, Jurnal Teknologi (Sci. Eng.), 74 (2015) 57–63.
[10] S.H. Tang, M.A.A. Zaini, Malachite green adsorption by potassium salts-activated carbons derived from textile sludge: equilibrium, kinetics and thermodynamics studies, Asia Pac. J. Chem. Eng., 12 (2017) 159–172.
[11] S. Wong, N.A.N. Yac'cob, N. Ngadi, O. Hassan, I.M. Inuwa, From pollutant to solution of wastewater pollution: synthesis of activated carbon from textile sludge for dye adsorption, Chin. J. Chem. Eng., 26 (2018) 870–878.
[12] J. Xue, Q. Cui, Y. Bai, Y. Wu, Y. Gao, L. Li, N. Qiao, Optimization of adsorption conditions for the removal of petroleum compounds from marine environment using modified activated carbon fiber by response surface methodology, Environ. Prog. Sustainable Energy, 35 (2016) 1400–1406.
[13] S.H. Tang, M.A.A. Zaini, Potassium hydroxide activation of activated carbon: a commentary, Carbon Lett., 16 (2015) 275–280.
[14] H. Wang, Y.N. Wang, Y. Sun, X. Pan, D. Zhang, Y.F. Tsang, Differences in Sb(V) and As(V) adsorption onto a poorly crystalline phyllomanganate (δ-MnO_2): adsorption kinetics, isotherms, and mechanisms, Process Saf. Environ., 113 (2018) 40–47.

[15] F. Gimbert, N. Morin-Crini, F. Renault, P.M. Badut, G. Crini, Adsorption isotherm models for dye removal by cationized starch-based material in a single component system: error analysis, J. Hazard. Mater., 157 (2008) 34–46.
[16] K.Y. Foo, B.H. Hameed, Insights into the modeling of adsorption isotherm systems, Chem. Eng. J., 156 (2010) 2–10.
[17] D. Prahas, Y. Kartika, N. Indraswati, S. Ismadji, Activated carbon from jackfruit peel waste by H_3PO_4 chemical activation: pore structure and surface chemistry characterization, Chem. Eng. J., 140 (2008) 32–42.
[18] A.O. Dada, A.P. Olalekan, A.M. Olatunya, O. Dada. Langmuir, Freundlich, Temkin and Dubinin–Radushkevich isotherms studies of equilibrium sorption of Zn^{2+} onto phosphoric acid modified rice husk. J. Appl. Chem., 3 (2012) 38–45.
[19] D.D. Maksin, S.O. Kljajević, M.B. Đolić, J.P. Marković, B.M. Ekmeščić, A.E. Onjia, A.B. Nastasović, Kinetic modeling of heavy metal sorption by vinyl pyridine based copolymer, Hemijska Industrija, 66 (2012) 795–804.
[20] B.H. Hameed, M.I. El-Khaiary, Equilibrium, kinetics and mechanism of malachite green adsorption on activated carbon prepared from bamboo by K_2CO_3 activation and subsequent gasification with CO_2, J. Hazard. Mater., 157 (2008) 344–351.
[21] A. Nasrullah, A.H. Bhat, A. Naeem, M.H. Isa, M. Danish, High surface area mesoporous activated carbon-alginate beads for efficient removal of methylene blue, Int. J. Biol. Macromol., 107 (2018) 1792–1799.
[22] F. Marrakchi, M.J. Ahmed, W.A. Khanday, M. Asif, B.H. Hameed, Mesoporous-activated carbon prepared from chitosan flakes via single-step sodium hydroxide activation for the adsorption of methylene blue, Int. J. Biol. Macromol., 98 (2017) 233–239.